USCAP

www.nature.com/modpathol

ARTICLE

Oncocytic renal neoplasms with diffuse keratin 7 immunohistochemistry harbor frequent alterations in the mammalian target of rapamycin pathway

Sambit K. Mohanty[1,2], Abhishek Satapathy[1], Aditi Aggarwal[2], Sourav K. Mishra[1], Nakul Y. Sampat[1], Shivani Sharma[2] and Sean R. Williamson[3]✉

Low-grade oncocytic tumor (LOT) has been recently proposed as a unique renal tumor. However, we have encountered tumors with more oncocytoma-like morphology that show diffuse keratin 7 reactivity, which we sought to characterize molecularly. Eighteen tumors with a diffuse keratin 7 positive and KIT negative pattern were identified from 184 with predominantly oncocytoma-like histology. These tumors were subjected to detailed immunohistochemical evaluation and 14 were evaluated using the Illumina® HiSeq 4000 platform for 324 cancer-associated genes. Patients' ages ranged from 39 to 80 (median = 59.5 years) with a male to female ratio of 1.25:1. Morphology was predominantly oncocytoma-like with discrete nests, compared to the solid and edematous patterns described in LOT. Other than positive keratin 7 and negative KIT, the tumor cells were positive for PAX8, E-cadherin, AE1/AE3, Ber-EP4, AMACR, CD10, and MOC31, and were negative for other studied markers. FH and INI1 were normal. Eleven of 14 harbored genomic abnormalities, likely sporadic, primarily involving the MTOR pathway (73%). Overall, the alterations included *MTOR* activating mutation ($n = 1$), *TSC1* inactivating mutation ($n = 1$), *TSC2* mutation (p.X534 splice site, $n = 1$), *STK11* (a negative regulator of the MTOR pathway) mutation ($n = 1$), both *STK11* and *TSC1* mutations ($n = 1$), biallelic loss of *PTEN* and *TSC1* deletion ($n = 1$), and *MET* amplification and *TSC1* inactivating mutation ($n = 1$). Amplification of *FGFR3* was identified in one additional tumor. Other alterations included *FOXP1* loss ($n = 1$), *NF2* E427 homozygous loss ($n = 1$), and *PI3KCA* activating mutation ($n = 1$). At a median follow-up of 68 months (2–147 months) for 15 patients, all were alive without disease. Oncocytic renal tumors with diffuse keratin 7 labeling show frequent alterations in the TSC/MTOR pathway, despite more oncocytoma-like morphology than initially described in LOT, likely expanding the morphologic spectrum of the latter.

Modern Pathology (2022) 35:361–375; https://doi.org/10.1038/s41379-021-00969-6

INTRODUCTION

Oncocytic renal tumors remain a common diagnostic challenge for the pathologist[1–5]. Whereas previously these included primarily oncocytoma and eosinophilic variant chromophobe renal cell carcinoma (ChrRCC), recent work has identified several recently established and emerging diagnostic entities based on key morphologic attributes, immunohistochemistry (IHC) and genomic profiles, and biologic behavior[6–13]. In general, low-grade oncocytic renal tumors are not aggressive neoplasms. They mostly portend an indolent clinical course with a good prognosis[14]. However, it has been recently recognized that some oncocytic renal neoplasms that have more ominous implications, such as succinate dehydrogenase-deficient RCC (which is hereditary) and rare examples of fumarate hydratase-deficient RCC that are deceptively low-grade with oncocytic features (which is hereditary and potentially more aggressive)[15–17]. Sometimes, the distinction between various categories of low-grade oncocytic renal neoplasm is not straightforward based on the morphology alone[2]. Keratin 7 and KIT are among the most common IHC markers employed to resolve this diagnostic dilemma. Although both oncocytoma and ChrRCC are usually KIT immunoreactive neoplasms, diffuse keratin 7 positivity would typically strongly favor ChrRCC. In contrast, keratin 7 is usually restricted to only occasional groups of cells in oncocytoma, constituting a very small percentage of the tumor cells[1]. Recently, low-grade oncocytic tumor (LOT) has been proposed as a potential entity in renal neoplasia that exhibits diffuse keratin 7 positivity with a negative result for KIT[18], differing from the expected phenotype of oncocytoma and showing more diffuse keratin 7 labeling than usually encountered in eosinophilic ChrRCC[18–20]. These have been found to have a distinct set of macroscopic and microscopic features characterized by a solitary, unilateral, unencapsulated, and well-circumscribed tumor mass with low-grade oncocytic cells arranged in a wide variety of architectural patterns. These tumors have some oncocytoma-like features and some features that argue against the diagnosis of oncocytoma. Oncocytoma-like features include lack of a well-formed capsule, diffuse solid growth pattern, compact nests at the periphery of the tumor, and tumor cells with uniformly abundant eosinophilic/oncocytic cytoplasm, and smooth contoured round to oval nuclei lacking significant nuclear irregularities. Other features including mosaic growth patterns and rarefied connective

[1]Department of Pathology and Laboratory Medicine, Advanced Medical Research Institute, Bhubaneswar, India. [2]Department of Pathology and Laboratory Medicine, CORE Diagnostics, Gurgaon, Haryana, India. [3]Department of Pathology, Cleveland Clinic, Cleveland, OH, USA. ✉email: williamson.sean@outlook.com

Received: 22 May 2021 Revised: 21 October 2021 Accepted: 25 October 2021
Published online: 20 November 2021

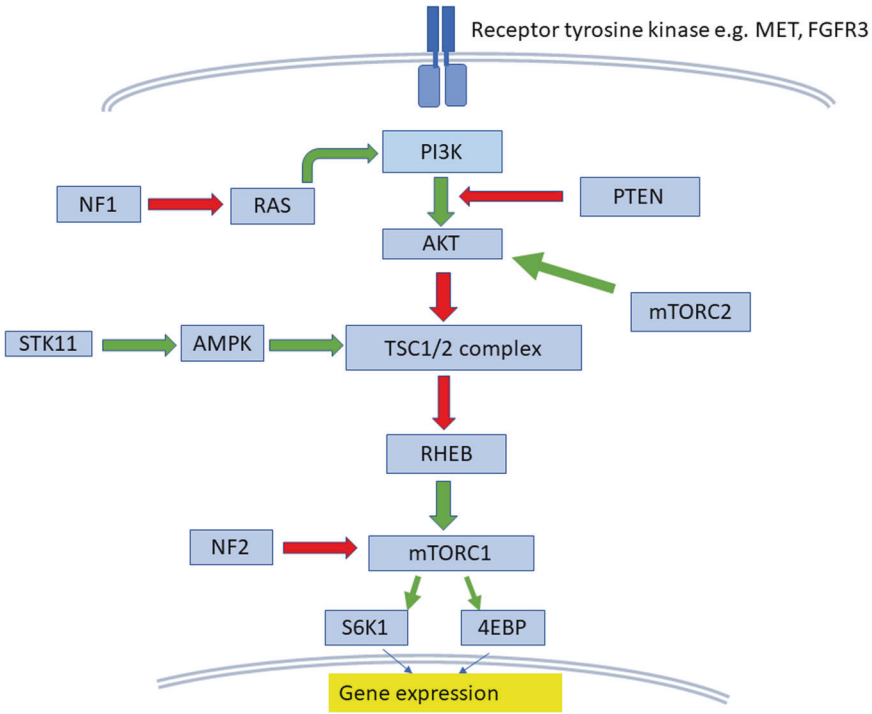

Fig. 1 MTORC1 complex is one of the master regulators of cell growth and metabolism. Its activity is regulated by the tuberous sclerosis complex (TSC). TSC is a GTPase activating protein (GAP). The GTPase protein RHEB regulates MTOR by increasing its activity. TSC inactivates RHEB and in turn downregulates MTOR activity. AMPK activates TSC complex, which in turn regulates the activity of MTOR. AKT signaling cascade is activated by receptor tyrosine kinases which induce production of phosphatidylinositol (3,4,5) trisphosphates (PIP3) by phosphoinositide 3-kinase (PI3K). NF1 protein, neurofibromin 1, negatively regulates RAS proteins through GTPase activity. Ras is an activator of the phosphatidylinositol-3-kinase (PI3K)-AKT pathway. The tumor suppressor phosphatase and tensin homolog (PTEN) inhibits AKT activity by dephosphorylating PIP3. AKT regulates cell growth through its effects on the TSC1/TSC2 complex and MTORC signaling.

tissue stroma with loosely arranged neoplastic cells distinct from the hypocellular zones of oncocytoma (compact cell islands and nests in the central area, described as archipelago-like pattern) and are sharply distinct from the solid areas, and the presence of delicate perinuclear halo/clearing argue against a diagnosis of oncocytoma. Since the number of cases of LOT studied to date is small, and these have likely been classified in the past under various terms, such as eosinophilic ChrRCC, oncocytic renal tumor, NOS, unclassified or LOT, hybrid oncocytoma-ChrRCC, borderline/uncertain/low malignant potential tumors, and so on, it is unclear what their true biologic behavior may be. Therefore, caution should be exercised in diagnosing oncocytoma when the typical features are not present.

We were particularly interested to study the TSC/MTOR (tuberous sclerosis complex/mammalian target of rapamycin) pathway in these neoplasms, as there is emerging evidence to suggest that LOT may be characterized by alterations in this pathway. For example, the Cancer Genome Atlas study of ChrRCC included at least 2 tumors with predominantly eosinophilic morphology that harbored mutations in *MTOR*[21]. Likewise, a few recent studies have found alterations in this pathway in neoplasms likely fitting the diagnostic criteria for LOT[22–25]. This is a key regulator pathway for wide array of vital cellular functions- cell metabolism, growth, proliferation, and survival[26–28]. The molecular weight of *MTOR* is 289 kDa and it belongs to the phosphoinositide 3-kinase related kinase family. It nucleates two multi-protein complexes MTORC1 and MTORC2. MTORC1 complex acts as one of the master regulators of cell growth and metabolism. Its activity is regulated by various growth factor pathways, environmental stress, nutritional, and oxygen status in the cell. The most important regulator is the TSC, which is a heterodimer of TSC1 (hamartin) and TSC2 (tuberin)[26]. TSC is a GTPase activating protein (GAP). The GTPase protein RHEB regulates MTOR by increasing its activity. TSC inactivates RHEB and in turn downregulates MTOR activity[29–31]. Activation of MTORC1 represses the PI3K-AKT pathway. Environmental stress results in the activation of AMP activated protein kinase (AMPK) by serine threonine kinase 11 (STK11). AMPK activates TSC1/TSC2 complex, which in turn regulates the activity of MTOR. MTORC2 depletion inhibits AKT, leading to decreased phosphorylation of forkhead box protein (FOXO1) and FOXO3A and their activation (Fig. 1).

We sought to study the morphologic and genetic characteristics of oncocytic tumors having low-grade features and keratin 7-positive/KIT-negative IHC profile from the archives of a single institution.

MATERIALS AND METHODS

Case selection criteria

This study was initiated on approval from the institutional review board. Tumors with predominantly renal oncocytoma-like morphology or subtle features of ChrRCC were included in the study. A total of 184 cases over a period of 9 years (January 2011 to April 2020) were selected. Among them, 18 renal tumors showing ISUP/WHO low-grade oncocytic morphology and diffuse positivity for keratin 7 and negativity for KIT were identified. Demographics, surgical procedure involved, type of specimen, macroscopic and microscopic features, and follow-up information were recorded in these cases.

All tissues were formalin-fixed and paraffin embedded (FFPE). Hematoxylin and eosin-stained sections were reviewed by three genitourinary pathologists (SKMo, SRW, and AS) to confirm the diagnosis.

Histochemical and immunohistochemical studies

Muller-Mowry colloidal iron stain was performed in 11 cases. The IHC stains performed were as follows: keratin 7 (Ventana Medical Systems: Clone SP52), KIT (Abcam, Polyclonal), PAX8 (Cell Marque; Polyclonal), alpha methyacyl CoA racemase (AMACR) (Cell Marque; Clone: 13H4), CD10 (Ventana Medical Systems; Clone: SP67), E-cadherin (Leica Biosystems; Clone: 36B5), keratin 20 (Biocare Medical, Clone: Ks20.8), carbonic anhydrase (CA) 9 (LS Bio; Clone: 303123), keratin AE1/AE3

Table 1. Demographics, types of surgical procedure, pathologic features, and follow-up information of the cohort.

Patient number	Age (years)	Gender	Procedure type	Laterality	Maximum dimension of the tumor (in mm) and focality	Macroscopic features	Histopathologic features	WHO/ISUP nuclear grade	Pathologic stage	Vital status	Follow-up (in months)
1	77	M	Radical nephrectomy	Left	60 and unifocal	Tan-brown and hemorrhagic	No capsule, well-circumscribed, and solid. Edematous stroma with nests, sheets, and trabeculae of tumor cells. Oncocytic round with smooth-contoured to slightly wrinkled nuclear envelope.	3	pT1b	ANED	118
2	39	M	Radical nephrectomy	Right	20 and unifocal	Tan-brown and solid; homogeneous	No capsule, well-circumscribed, and solid. Edematous stroma with nests, sheets, and trabeculae of tumor cells. Oncocytic round with smooth-contoured nuclear envelope.	3	pT1a	ANED	57
3	65	F	Partial nephrectomy	Left	23 and unifocal	Tan-brown and solid; homogeneous	No capsule, well-circumscribed, and solid. Edematous stroma with nests, sheets, tubules (focally), and trabeculae of tumor cells. Eosinophilic round with smooth-contoured to slightly wrinkled nuclear envelope.	3	pT1a	ANED	2
4	50	M	Radical nephrectomy	Left	42 and unifocal	Tan-brown and solid; homogeneous	No capsule, well-circumscribed, and solid. Edematous stroma with nests, sheets, and trabeculae of tumor cells. Oncocytic round with smooth-contoured nuclear envelope.	2	pT1b	LTF	LTF

Table 1 continued

Patient number	Age (years)	Gender	Procedure type	Laterality	Maximum dimension of the tumor (in mm) and focality	Macroscopic features	Histopathologic features	WHO/ISUP nuclear grade	Pathologic stage	Vital status	Follow-up (in months)
5	42	M	Radical nephrectomy	Right	38 and unifocal	Tan-brown and solid; homogeneous	No capsule, well-circumscribed, and solid. Edematous stroma with nests, sheets, and trabeculae of tumor cells. Oncocytic round with smooth-contoured nuclear envelope.	3	pT1a	ANED	103
6	75	M	Radical nephrectomy	Right	70 and unifocal	Tan-brown and solid; homogeneous with focal tan-white areas	No capsule, well-circumscribed, and solid. Edematous stroma with nests, sheets, and trabeculae of tumor cells. Oncocytic round with smooth-contoured nuclear envelope. Focal degenerative nuclear features.	2	pT3a	ANED	49
7	60	F	Radical nephrectomy	Right	21 and unifocal	Tan-brown and solid; homogeneous	No capsule, well-circumscribed, and solid. Edematous stroma with nests, sheets, and trabeculae of tumor cells. Oncocytic round with smooth-contoured nuclear envelope.	2	pT1a	ANED	52
8	53	F	Radical nephrectomy	Left	107 and unifocal	Tan-brown and solid; homogeneous	No capsule, well-circumscribed, and solid. Edematous stroma with nests, sheets, and trabeculae of tumor cells. Oncocytic round with smooth-contoured nuclear envelope.	3	pT2b	ANED	68

Table 1 continued

Patient number	Age (years)	Gender	Procedure type	Laterality	Maximum dimension of the tumor (in mm) and focality	Macroscopic features	Histopathologic features	WHO/ISUP nuclear grade	Pathologic stage	Vital status	Follow-up (in months)
9	69	M	Radical nephrectomy	Right	30 and unifocal	Tan-brown and solid; homogeneous	No capsule, well-circumscribed, and solid. Edematous stroma with nests, sheets, and trabeculae of tumor cells. Oncocytic round with smooth-contoured nuclear envelope. Focal degenerative nuclear features.	3	pT1a	ANED	7
10	40	F	Radical nephrectomy	Right	93 and unifocal	Tan-brown and solid; homogeneous	No capsule, well-circumscribed, and solid. Edematous stroma with nests, sheets, and trabeculae of tumor cells. Oncocytic round with smooth-contoured nuclear envelope.	3	pT2a	ANED	11
11	61	F	Radical nephrectomy	Right	18 and unifocal	Tan-brown and solid; homogeneous	No capsule, well-circumscribed, and solid. Edematous stroma with nests, sheets, and trabeculae of tumor cells. Oncocytic round with smooth-contoured nuclear envelope.	2	pT1a	ANED	75
12	44	F	Radical nephrectomy	Left	32 and unifocal	Tan-brown and solid; homogeneous	No capsule, well-circumscribed, and solid. Edematous stroma with nests, sheets, tubular, cords, and trabeculae of tumor cells. Oncocytic round with smooth-contoured nuclear envelope. Focal	2	pT1a	ANED	138

Table 1 continued

Patient number	Age (years)	Gender	Procedure type	Laterality	Maximum dimension of the tumor (in mm) and focality	Macroscopic features	Histopathologic features	WHO/ISUP nuclear grade	Pathologic stage	Vital status	Follow-up (in months)
							degenerative nuclear features.				
13	59	M	Radical nephrectomy	Right	14 and unifocal	Tan-brown and solid; homogeneous	No capsule, well-circumscribed, and solid. Edematous stroma with nests, sheets, cords, reticular, and trabeculae of tumor cells. Eosinophilic round with smooth-contoured nuclear envelope.	3	pT1a	ANED	55
14	71	F	Radical nephrectomy	Right	29 and unifocal	Tan-brown and solid; homogeneous	No capsule, well-circumscribed, and solid. Edematous stroma with nests, sheets, and trabeculae of tumor cells. Eosinophilic round with smooth-contoured nuclear envelope.	2	pT1a	ANED	101
15	65	M	Radical nephrectomy	Left	17 and unifocal	Tan-brown and solid; homogeneous with focal tan-white thin strands	No capsule, well-circumscribed, and solid. Edematous stroma with nests, sheets, and trabeculae of tumor cells. Eosinophilic round with smooth-contoured nuclear envelope.	2	pT1a	LTF	LTF
16	49	F	Partial nephrectomy	Left	30 and unifocal	Tan-brown and solid; homogeneous	No capsule, well-circumscribed, and solid. Edematous stroma with nests, sheets, and trabeculae of tumor cells. Eosinophilic round with smooth-contoured nuclear envelope.	3	pT1a	ANED	112

Table 1 continued

Patient number	Age (years)	Gender	Procedure type	Laterality	Maximum dimension of the tumor (in mm) and focality	Macroscopic features	Histopathologic features	WHO/ISUP nuclear grade	Pathologic stage	Vital status	Follow-up (in months)
17	57	M	Radical nephrectomy	Right	23 and unifocal	Tan-brown and solid; homogeneous with focal hemorrhage	No capsule, well-circumscribed, and solid. Edematous stroma with nests, sheets, and trabeculae of tumor cells. Eosinophilic round with smooth-contoured nuclear envelope.	3	pT1a	ANED	147
18	80	M	Partial nephrectomy	Left	20 and unifocal	Tan-brown and solid; homogeneous	No capsule, well-circumscribed, and solid. Edematous stroma with nests, sheets, and trabeculae of tumor cells. Oncocytic round with smooth-contoured nuclear envelope.	3	pT1a	LTF	LTF

ANED alive with no evidence of disease, *LTF* lost to follow-up.

(Ventana Medical Systems; Clone: AE1/AE3), vimentin (Ventana Medical Systems; Clone: V9), EPCAM (Biocare Medical; Clone: Ber-EP4), MOC31 (Biocare Medical; Clone: MOC31), Ki-67 (Biocare Medical; Clone: MIB 1), keratin 5/6 (Ventana Medical Systems; Clone: D5), melanosome (Ventana Medical Systems; Clone: HMB-45), melan A (Ventana Medical Systems; Clone: A103), INI1 (SMARCB1, Ventana Medical Systems; Clone: MRQ-27), CD15 (Ventana Medical Systems; Clone: MMA), inhibin (Cell Marque; Clone: MRQ-63), FH (Santa Cruz Biotechnology; Clone: J-13), p63 (Ventana Medical Systems; Clone: 4A4), and PD-L1 (Ventana Medical Systems; Clone: SP263). Four micrometer sections were prepared for IHC. Ventana Benchmark ULTRA autoimmunostainer. Cell conditioning 1 at high pH (pH = 8) was used for the antigen retrieval buffer solution and UltraView DAB Detection Kit was used the detection of the IHC product. Appropriate positive and negative controls were performed with each antibody. The results of the IHC stains were recorded in a semiquantitative fashion as described below.

Positive staining was defined as cytoplasmic and membranous (keratin 7, KIT, AMACR, CD10, E-cadherin, keratin 20, CA9, pan keratin, vimentin, Ber-EP4, MOC31, HMB-45, melan A, CD15, inhibin, PD-L1 [membranous]) or nuclear (PAX8 and p63) staining pattern in the tumor cells, which can be easily observed at low power magnification (×<40). Scant fine granular background staining of the tumor cells, which cannot be seen at low power magnification, or no staining at all was considered negative. For each case, immunoreactivity was interpreted as follows: negative ≤ 5% tumor cell staining; positive = ≥ 5% tumor cell staining. The percentages of immunoreactivity for these markers were evaluated in a semiquantitative fashion as follows: 0 ≤ 5% tumor cell staining; focal = 5–10% tumor cell staining; multifocal = 11–50% tumor cell staining; diffuse ≥ 50% tumor cell staining. The intensity of immunoreactivity was graded as weak, moderate, and strong.

MIB1 (Ki-67) demonstrated nuclear immunoreactivity and aided in evaluation of the proliferation index. The results were expressed in a semiquantitative manner as estimated percentage of tumor cells immunoreactive with the antibodies. A MIB1 (Ki-67) proliferation index (% positivity in 100 cells counted) was ascertained for each case. INI1 depicted nuclear positivity. Approximate percentage of INI1 positive nuclei were recorded in each case. It was considered as 'retained' (normal) if the majority of the nuclei showed positivity. FH showed cytoplasmic positivity. Percentage of cells retaining this IHC was noted for each case.

Molecular analysis

Targeted NGS panel. FFPE tumor tissue blocks of the selected tumor specimens were used for molecular evaluation using targeted NGS-based panel to detect small nucleotide variants/substitutions, small indels (insertions and/or deletions), and copy number variations in 324 cancer-associated genes (including genes involved in PI3K/AKT/MTOR pathway). The panel also detects selected gene rearrangements as well as genomic signatures including microsatellite instability and tumor mutational burden. The panel was based on Illumina® HiSeq 4000 platform.

Pathological evaluation of clinical specimens. Paraffin sections from the FFPE blocks were stained with H&E-stain for pathological evaluation, and FFPE tissue blocks that had at least 15% of tumor content were selected. Molecular analysis was performed in 14 cases.

DNA extraction. DNA was extracted from the selected FFPE blocks using the GeneREAD DNA FFPE kit (Qiagen) following the manufacturer's instruction. Then DNA was quantified by using Qubit 1XdsDNA high sensitivity assay.

Construction of libraries. DNA (50–1000 ng) was used for whole-genome shotgun library construction and hybridization-based capture of all coding exons from 309 cancer-related genes, one promoter region, one non-coding (ncRNA), and select intronic regions from 34 commonly rearranged genes, 21 of which also include the coding exons. In total, the assay detects alterations in a total of 324 genes.

Sequencing. Using the Illumina® HiSeq 4000 platform, hybrid capture-selected libraries were sequenced to high uniform depth (targeting ×500 median coverage with 99% of exons at coverage ×100).

Sequence data processing. Sequence data was then processed using a customized analysis pipeline. Low-quality data was filtered out and the output BAM files were aligned to the human reference genome hg19. Variant calling pipeline was then called all the variants that has passed various QC checks, including strand bias, minor allele frequency (MAF), Q score, depth of coverage (×500), Phred quality score, noise in the surrounding region etc. The variants were then segregated on the basis of their genomic location and variant

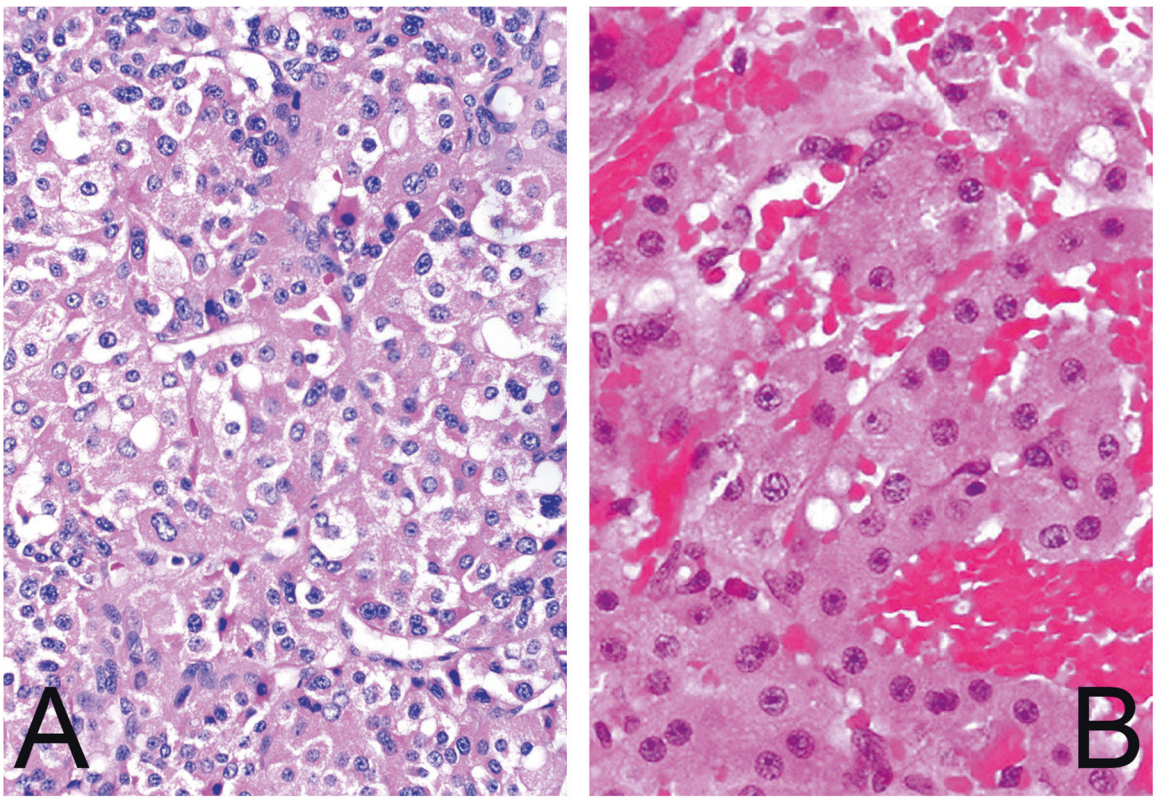

Fig. 2 Histologic features of the tumors. Histology of the tumors was predominantly oncocytoma-like, often having compact (**A**) architecture, with round, regular nuclei (**B**).

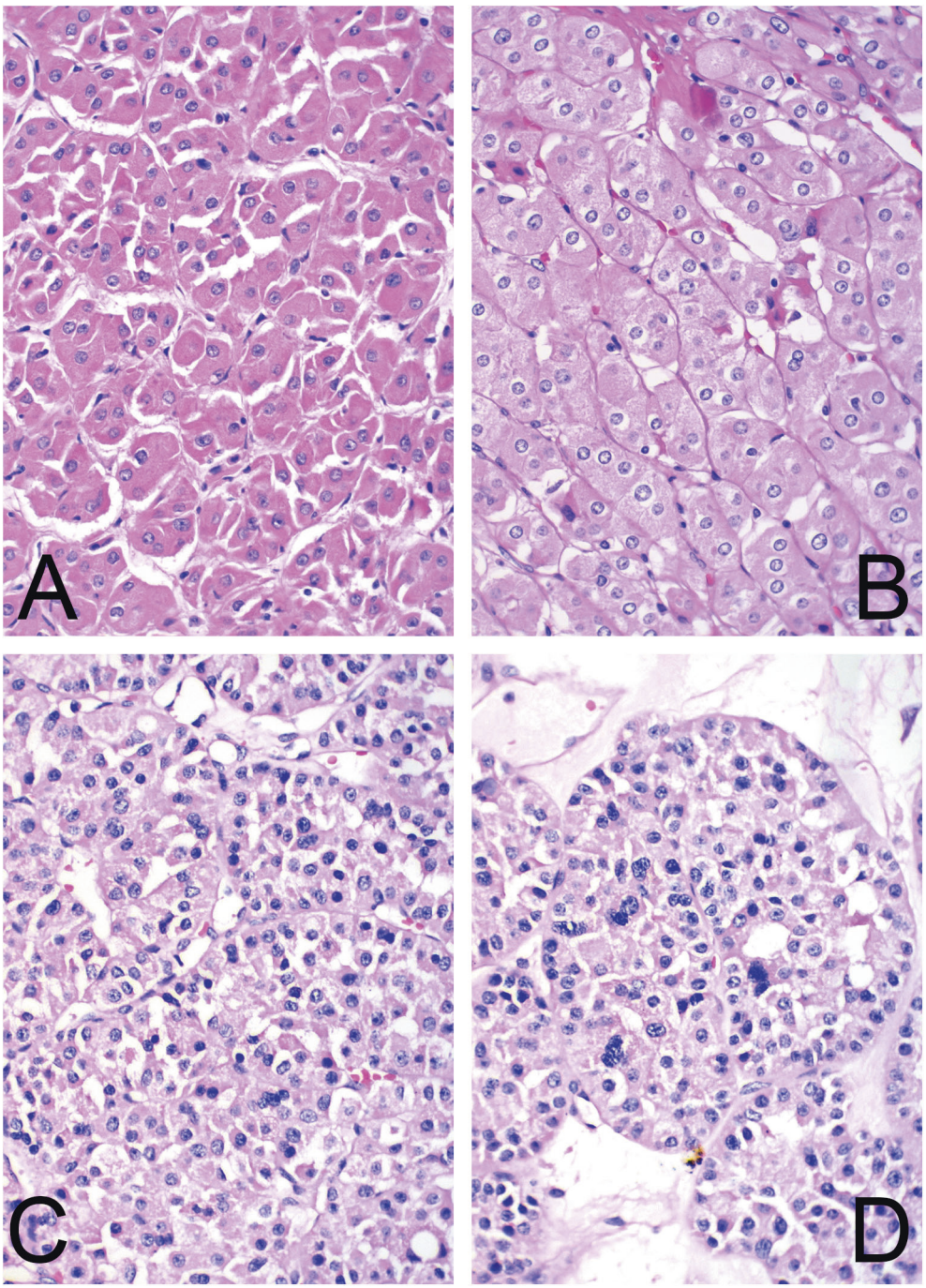

Fig. 3 Variations in the nuclear and architectural features of the tumors. These included: abundant fine granular eosinophilic cytoplasm with round to oval nuclei, resembling what has been described in LOT (**A**). Occasional tumors showed minor perinuclear clearing (**B**). Minor nuclear membrane irregularity was noted in a subset of cells (**C**), and some tumors showed degenerative nuclear atypia, as seen in some oncocytomas (**D**).

effects (missense, non-frameshift, and frameshift insertions, deletions, and base substitutions). Variant annotation was performed using the Association for Molecular Pathology classification.

RESULTS

Clinical features

There were 18 patients that satisfied the criteria and were included in the study. The patients' ages ranged from 39 years to 80 years (mean = 56.5 years; median = 59.5 years) at the time of diagnosis. A slight male preponderance was observed with 56% of the total patients (10/18) being male. Unilateral solitary renal mass was observed in every patient (right, $n = 10$; left, $n = 8$). No other mass was present concurrently in any of the patients. There was neither any notable family or personal history of malignancy, nor any syndromic association. The patients had undergone either partial nephrectomy ($n = 3$) or total nephrectomy ($n = 15$) (Table 1).

Macroscopic features

On gross examination, the maximum dimension of the tumors ranged from 14 to 107 mm (median = 29.5 mm; mean = 37.1 mm).

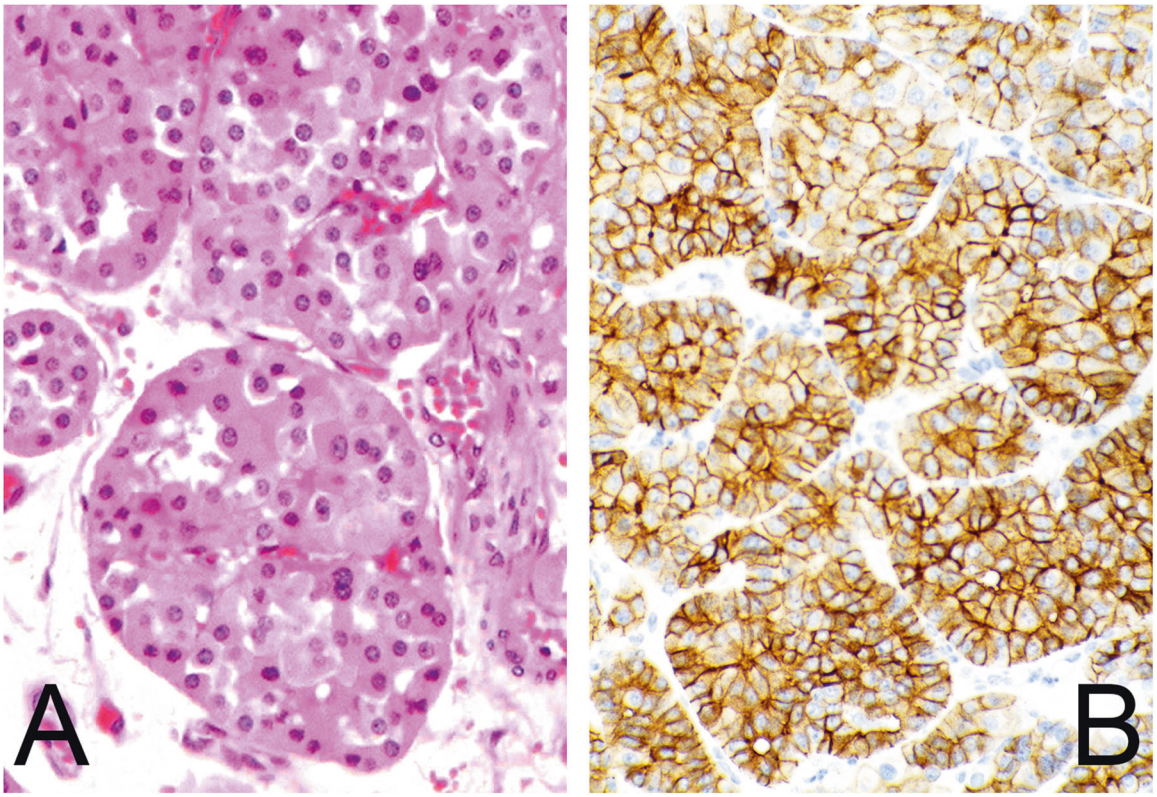

Fig. 4 Immunohistochemistry in the tumors. This tumor shows predominantly oncocytoma-like nests (**A**). Keratin 7 staining shows diffuse positivity with membranous accentuation (**B**).

The tumors were unilateral, solitary, and unencapsulated but well-circumscribed. The cut surfaces were homogeneous and tan-brown in all tumors. One tumor had focal tan-white area and two had focal areas of hemorrhage. No cystic, tan-yellow/yellow, or overtly friable necrotic areas was observed in any of the tumors (Table 1).

Microscopic features

The tumors were unencapsulated but well-circumscribed. Predominant morphology was oncocytoma-like with frequent and repetitive nested appearance. A variety of other growth patterns was observed that include solid, nested, reticular, sheets, tubular, trabecular, and cord-like. The stroma was edematous and was sharply demarcated from the cellular tumor areas. Fibrous stroma was also observed. The neoplastic cells were round to polygonal. They had homogenous abundant fine granular eosinophilic cytoplasm with round to oval nuclei. No frank nuclear envelope irregularity or perinuclear clearing was identified, except for two tumors where mildly wrinkled (raisinoid) nuclear membrane was observed. Degenerative nuclear atypia was seen in three tumors. The nucleoli were small and delicate to conspicuous. The ISUP/WHO nuclear grades were as follows: grade 2, $n = 7$; grade 3, $n = 11$ (Figs. 2 and 3 and Table 1).

Immunohistochemical features

All the tumors were positive for keratin 7 and negative for KIT by the study selection criteria (Fig. 4). The keratin 7 expression was diffuse and strong in all 18 tumors. Other positive stains were as follows: PAX8 (16/16), E-cadherin (16/16), keratin AE1/AE3(18/18), Ber-EP4 (14/14), and MOC31 (16/16). The expression ranged from moderate to strong in the intensity and focal to diffuse in the extent. Three of eighteen tumors showed weak and focal AMACR expression. CD10 was expressed in a moderate to focal manner in 3 of 18 tumors. keratin 20 (0/18), CA9 (0/18), vimentin (0/18), keratin 5/6 (0/18), HMB-45 (0/17), melan A (0/18), CD15 (0/18), inhibin (0/10), and p63 (0/17) were negative. FH (12/12) and INI1 (18/18) were retained/normal in the tumor cells. Ki-67 labeling index varied between 2 and 7%. PD-L1 was performed in six tumors and all were negative. Colloidal iron Muller-Mowry stain depicted a negative result (0/11) when performed (Table 2a and b).

Molecular analysis features

Eleven of fourteen tumors harbored genomic abnormalities, as shown in Table 3 and Fig. 5. The mutations were primarily involving the MTOR pathway in eight tumors (73%). *TSC1* inactivating mutation and deletion was identified in two and one tumors, respectively. *TSC2* mutation (p.X534 splice site) was seen in one tumor. *STK11*, a negative regulator of the MTOR pathway, was mutated in two tumors. Amplifications of *MET* and *FGFR3* genes were identified in one tumor each. Other mutations observed were biallelic loss of *PTEN* ($n = 1$), *FOXP1* loss ($n = 1$), *NF2* E427 homozygous loss ($n = 1$), and *PI3KCA* activating mutation ($n = 1$). One tumor had both *STK11* and *TSC1* mutations and another tumor had biallelic loss of *PTEN* and *TSC1* deletion. *MET* amplification and *TSC1* inactivating mutation was seen in one tumor (Table 3 and Fig. 5). Comparison to the adjacent normal tissue was performed in all the 14 tumors, in which the alterations were identified in tumor tissue only, arguing against germline alterations.

Staging, follow-up, and survival information

Assuming application of the 8th edition AJCC TNM system to these tumors, as they do not meet definite criteria for oncocytoma, most of the tumors would be regarded as low-stage: 72% of the tumors (13/18) were of stage pT1a, 11% (2/18) pT1b, 6% (1/18) each was pT2a, pT2b, and pT3a. Follow-up data was available in 15 cases. The follow-up period ranged from 2 months to 147 months, with a median of 68 months. All the

Table 2. (a) Immunohistochemical characteristics of the tumors in the cohort. (b) Immunohistochemical characteristics of the tumors in the cohort.

(a)

Patient number	PAX8	AMACR	CD10	KIT/CD117	E-Cadherin	KRT7	KRT20	CA9	AE1/AE3	Vimentin	Ber-EP4	MOC31
1	Pos	Neg	Neg	Neg	Pos	Pos	Neg	Neg	Pos	Neg	Pos	Pos
2	Pos	Focal and weak	Neg	Neg	Pos	Pos	Neg	Neg	Pos	Neg	Pos	Not done
3	Pos	Neg	Focal	Neg	Pos	Pos	Neg	Neg	Pos	Neg	Pos	Not done
4	Pos	Neg	Neg	Neg	Pos	Pos	Neg	Neg	Pos	Neg	Pos	Pos
5	Pos	Neg	Neg	Neg	Pos	Pos	Neg	Neg	Pos	Neg	Pos	Pos
6	Pos	Focal	Neg	Neg	Pos	Pos	Neg	Neg	Pos	Neg	Pos	Pos
7	Pos	Neg	Neg	Neg	Pos	Pos	Neg	Neg	Pos	Neg	Not done	Pos
8	Pos	Neg	Neg	Neg	Pos	Pos	Neg	Neg	Pos	Neg	Pos	Pos
9	Pos	Neg	Focal	Neg	Pos	Pos	Neg	Neg	Pos	Neg	Pos	Pos
10	Pos	Neg	Neg	Neg	Pos	Pos	Neg	Neg	Pos	Neg	Pos	Pos
11	Pos	Neg	Neg	Neg	Pos	Pos	Neg	Neg	Pos	Neg	Pos	Pos
12	Pos	Neg	Neg	Neg	Pos	Pos	Neg	Neg	Pos	Neg	Not done	Pos
13	Pos	Neg	Focal and weak	Neg	Pos	Pos	Neg	Neg	Pos	Neg	Not done	Pos
14	Pos	Neg	Neg	Neg	Not done	Pos	Neg	Neg	Pos	Neg	Pos	Pos
15	Pos	Weak	Neg	Neg	Not done	Pos	Neg	Neg	Pos	Neg	Pos	Pos
16	Pos	Not done	Neg	Neg	Pos	Pos	Neg	Neg	Pos	Neg	Not done	Pos
17	Pos	Neg	Neg	Neg	Pos	Pos	Neg	Neg	Pos	Neg	Pos	Pos
18	Pos	Not done	Neg	Neg	Pos	Pos	Neg	Neg	Pos	Neg	Pos	Pos

(b)

Patient number	Ki-67	KRT5/6	HMB-45	Melan A	INI1	CD15	Inhibin	FH	p63	PD-L1 (SP263)
1	2%	Neg	Neg	Neg	Retained	Neg	Neg	Not done	Not done	Not done
2	3%	Neg	Not done	Neg	Retained	Neg	Not done	Retained	Neg	Not done
3	5%	Neg	Neg	Neg	Retained	Neg	Neg	Retained	Neg	0
4	7%	Neg	Neg	Neg	Retained	Neg	Not done	Not done	Neg	0
5	2%	Neg	Neg	Neg	Retained	Neg	Not done	Retained	Neg	Not done
6	2%	Neg	Neg	Neg	Retained	Neg	Neg	Not done	Neg	0
7	5%	Neg	Neg	Neg	Retained	Neg	Not done	Retained	Neg	Not done
8	2%	Neg	Neg	Neg	Retained	Neg	Neg	Retained	Neg	0
9	2%	Neg	Neg	Neg	Retained	Neg	Neg	Retained	Neg	Not done
10	5%	Neg	Neg	Neg	Retained	Neg	Neg	Not done	Neg	0
11	2%	Neg	Neg	Neg	Retained	Neg	Neg	Retained	Neg	Not done
12	5%	Neg	Neg	Neg	Retained	Neg	Neg	Retained	Neg	0
13	2%	Neg	Neg	Neg	Retained	Neg	Neg	Retained	Neg	0
14	2%	Neg	Neg	Neg	Retained	Neg	Neg	Not done	Neg	Not done
15	2%	Neg	Neg	Neg	Retained	Neg	Not done	Retained	Neg	Not done

Table 2 continued

(b)

Patient number	Ki-67	KRT5/6	HMB-45	Melan A	INI1	CD15	Inhibin	FH	p63	PD-L1 (SP263)
16	5%	Neg	Neg	Neg	Retained	Neg	Not done	Retained	Neg	Not done
17	5%	Neg	Neg	Neg	Retained	Neg	Not done	Not done	Neg	Not done
18	5%	Neg	Neg	Neg	Retained	Neg	Not done	Retained	Neg	Not done

(a) *KRT* keratin, *CA* carbonic anhydrase, *Pos* positive, *Neg* negative.
(b) *Pos* positive, *Neg* negative, *FH* fumarate hydratase, *PD-L* programmed death ligand-1.

patients were alive without evidence of recurrent renal tumor (Table 1).

DISCUSSION

Classifying oncocytic renal tumors into one of two categories—ChrRCC and oncocytoma—remains challenging. In general, the anticipated IHC pattern of oncocytoma is membranous KIT positivity, sometimes weak, and either a negative or focal/occasional keratin 7 positive profile. However, LOT has been recently described as a potentially distinct group, being negative for KIT, yet with diffuse positivity for keratin 7[18]. In this study, we hypothesized that LOT may be characterized by MTOR pathway alterations; however, we found diffuse keratin 7 reactivity and enriched somatic mutation of the TSC/MTOR pathway genes in a broader than expected spectrum of tumors with oncocytoma-like morphology.

According to previous reports, LOT exhibits morphology that primarily includes a solid sheet-like pattern, compact nested appearance, trabecular arrangement, tubule formation, reticular growth, and various intermediate areas with variable cellularity. A key helpful clue to recognition of this entity is that the stroma is often loose and edematous, with tumor cells that appear "stretched" or loosely connected to one another, contrasting to the discrete round nests typical of oncocytoma[18]. However, in this series, we encountered diffuse keratin 7 labeling in a cohort of tumors with predominantly nested oncocytoma-like morphology. Worrisome features pointing towards a diagnosis of malignancy, such as pleomorphism, mitotic activity, and/or coagulative necrosis were lacking. Most of the tumors in our cohort were small and confined to the kidney.

The molecular alterations in LOTs have not been studied in detail in the existing literature. Molecularly, oncocytomas generally have minimal/rare chromosomal abnormalities. They usually have diploid karyotype. In some other instances, they show loss of chromosome 1, loss of Y, or rearrangement of 11q13[1]. On the other hand, eosinophilic ChrRCCs have significantly greater extent of chromosomal aberrations characterized frequently by multiple losses of chromosomes[1,32]. Both oncocytoma and ChrRCC display mitochondrial gene mutations[33]. Reported "hybrid" tumors may show a mixture gains and losses of the chromosomes[34]. Initial studies of LOT suggest different karyotypic patterns, including a similar karyotype to that of oncocytoma. Our study sought to find out any unique abnormality at the genomic level.

Genomic analyses were performed in 14 tumors, in which alterations in the TSC/MTOR pathway was enriched. Various genetic alterations found are depicted in the Table 3 and Fig. 5. Abnormal MTOR signaling can result from the genetic aberrations in various levels, both upstream and downstream effectors. Increased activity of the MTOR results in cellular proliferation and metabolism that can lead to tumorigenesis. Theoretically, this tumor subtype could potentially be targeted by MTOR inhibitors, assuming that malignant behavior necessitates it, or large tumor size becomes worrisome in a patient that is not a candidate for surgery; however, to date these tumors appear nonaggressive, making necessity of targeted therapy likely rare.

MTOR pathway aberration is not unique to this group of renal neoplasms. Various other renal neoplasms such as eosinophilic solid and cystic RCC and eosinophilic vacuolated tumor have also shown these molecular alterations[35]. This common molecular alteration has made us wonder, if the tumors studied herein should be considered part of the spectrum of LOT, according to their shared genomics, despite differing morphologic patterns. At present, it seems that this should expand the spectrum of LOT, to include architecture that is more oncocytoma-like. As such, it would likely be prudent to ascertain the keratin 7 and KIT status in low-grade oncocytic neoplasms including possible oncocytomas, given the overlapping histomorphology of LOT. This would aid in

Table 3. Genomic alterations of the tumors in the cohort.

Patient number	Gene symbol	Gene name	Transcript ID	Variant annotation (p.)	Variant annotation (c.DNA)	Pathogenic role	Allelic frequency
1			NA	NA	NA	NA	NA
2	*STK11*	Serine/threonine kinase 11	NM_000455.4	p.?	c.921-1G>C	Pathogenic	22.2%
	TSC1	Tuberous sclerosis 1	NM_000368.4	p.Glu876Ter	c.2626G>T	Pathogenic	15%
3	*MTOR*	Mammalian target of rapamycin	NM_004958.4	p.Leu2427Arg	c.7281G>A	Pathogenic	29%
4	*FGFR3*	Fibroblast growth factor receptor 3	NM_001163213	Amplification	Amplification	Pathogenic	27.3%
5			NA	NA	NA	NA	
6	*NF2*	Neurofibromin 2	NM_000268.4	p.Glu427Ter	c.?	Pathogenic	35.5%
7	*PTEN*	Phosphatase and tensin homolog	NM_000314.8	Biallelic loss del (1p36.33)	Biallelic loss del (1p36.33)	Pathogenic	99%
	TSC1	Tuberous sclerosis 1	NM_000368.4	Allelic loss 9q34.13	Allelic loss 9q34.13	Pathogenic	45%
8	*MET*	MET receptor tyrosine kinase gene	NM_000245.4	Amplification	Amplification	Pathogenic	43%
	TSC1	Tuberous sclerosis 1	NM_000368.4	p.Glu876Ter	c.2626G>T	Pathogenic	11.9%
9	*TSC1*	Tuberous sclerosis 1	NM_000368.4	p.Glu876Ter	c.2626G>T	Pathogenic	20%
10	*PIK3CA*	Phosphatidylinositol-4,5-bisphosphate 3-kinase catalytic subunit alpha	NM_006218.4	p.Glu545Lys	c.1633G>A	Pathogenic	28.6%
11	*STK11*	Serine/threonine kinase 11	NM_000455.4	p.?	c.921-1G>C	Pathogenic	9.5%
12	*TSC2*	Tuberous sclerosis 2	NM_000548	p.Val534Leu	c.1600G>T	Pathogenic	31.7%
13			NA	NA	NA	NA	
14	*FOXP1*	Forkhead box P1	NM_001349338.3	p.Glu490Ter	c.1468G>T	Pathogenic	17.5%

NA not applicable.

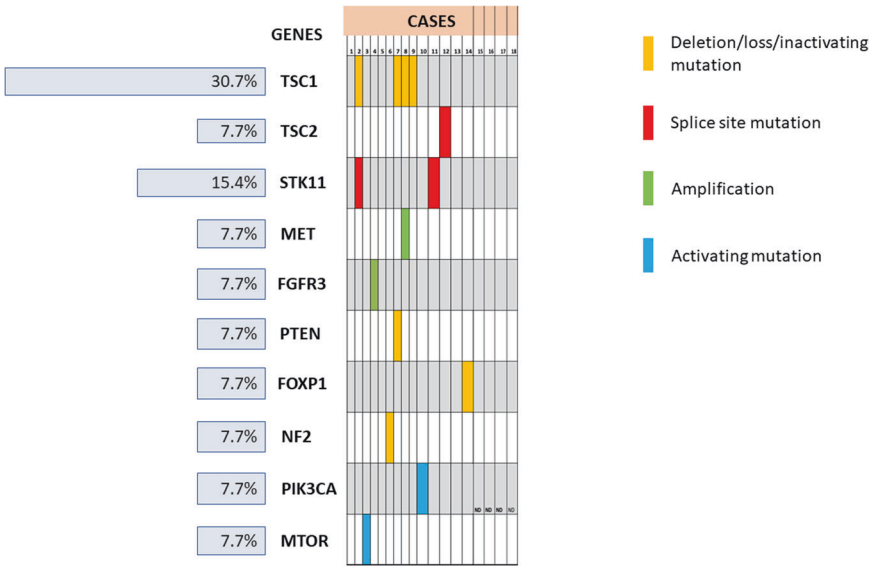

Fig. 5 Genomic profile of the tumors in the cohort. Genetic alterations are shown by colored bars.

differentiating a well characterized benign neoplasm from LOT, which is less clearly understood and requires further study. Nonetheless, it is likely that the behavior of all these oncocytic neoplasms is highly favorable, given that there remains considerable debate in optimal diagnostic criteria and most of these have almost certainly been historically diagnosed as variations of oncocytoma or eosinophilic ChrRCC in the past.

DATA AVAILABILITY

Raw data is available from the corresponding author upon reasonable request.

REFERENCES

1. Wobker, S. E. & Williamson, S. R. Modern pathologic diagnosis of renal oncocytoma. *J. Kidney Cancer VHL* **4**, 1–12 (2017).
2. Williamson, S. R. et al. Diagnostic criteria for oncocytic renal neoplasms: a survey of urologic pathologists. *Hum. Pathol.* **63**, 149–156 (2017).
3. Ng, K. L. et al. A systematic review and meta-analysis of immunohistochemical biomarkers that differentiate chromophobe renal cell carcinoma from renal oncocytoma. *J. Clin. Pathol.* **69**, 661–671 (2016).
4. Ng, K. L. et al. Differentiation of oncocytoma from chromophobe renal cell carcinoma (RCC): can novel molecular biomarkers help solve an old problem? *J. Clin. Pathol.* **67**, 97–104 (2014).
5. Kryvenko, O. N., Jorda, M., Argani, P. & Epstein, J. I. Diagnostic approach to eosinophilic renal neoplasms. *Arch. Pathol. Lab. Med.* **138**, 1531–1541 (2014).
6. Mehra, R. et al. Somatic bi-allelic loss of TSC genes in eosinophilic solid and cystic renal cell carcinoma. *Eur. Urol.* **74**, 483–486 (2018).
7. Palsgrove, D. N. et al. Eosinophilic solid and cystic (ESC) renal cell carcinomas harbor TSC mutations: molecular analysis supports an expanding clinicopathologic spectrum. *Am. J. Surg. Pathol.* **42**, 1166–1181 (2018).
8. Parilla, M. et al. Are sporadic eosinophilic solid and cystic renal cell carcinomas characterized by somatic tuberous sclerosis gene mutations? *Am. J. Surg. Pathol.* **42**, 911–917 (2018).
9. Trpkov, K. et al. Eosinophilic, Solid, and Cystic Renal Cell Carcinoma: Clinicopathologic Study of 16 Unique, Sporadic Neoplasms Occurring in Women. *Am. J. Surg. Pathol.* **40**, 60–71 (2016).
10. Chen, Y. B. et al. Somatic mutations of TSC2 or MTOR characterize a morphologically distinct subset of sporadic renal cell carcinoma with eosinophilic and vacuolated cytoplasm. *Am. J. Surg. Pathol.* **43**, 121–131 (2019).
11. He, H. et al. "High-grade oncocytic renal tumor": morphologic, immunohistochemical, and molecular genetic study of 14 cases. *Virchows Arch.* **473**, 725–738 (2018).
12. Siadat, F. & Trpkov, K. ESC, ALK, HOT and LOT: Three Letter Acronyms of Emerging Renal Entities Knocking on the Door of the WHO Classification. *Cancers* **12**, 168 (2020).
13. Trpkov, K. & Hes, O. New and emerging renal entities: a perspective post-WHO 2016 classification. *Histopathology* **74**, 31–59 (2019).
14. Richard, P. O. et al. Active surveillance for renal neoplasms with oncocytic features is safe. *J. Urol.* **195**, 581–586 (2016).
15. Smith, S. C. et al. A distinctive, low-grade oncocytic fumarate hydratase-deficient renal cell carcinoma, morphologically reminiscent of succinate dehydrogenase-deficient renal cell carcinoma. *Histopathology* **71**, 42–52 (2017).
16. Gill, A. J. Succinate dehydrogenase (SDH)-deficient neoplasia. *Histopathology* **72**, 106–116 (2018).
17. Gill, et al. Succinate dehydrogenase-deficient renal carcinoma. In *WHO Classification of Tumours of the Urinary System and Male Genital Organs* Vol. 8 (eds Moch, H., Humphrey, P. A., Ulbright T. M., & Reuter, V. E.) 35–36 (International Agency for Research on Cancer, Lyon, 2016).
18. Trpkov, K. et al. Low-grade oncocytic tumour of kidney (CD117-negative, cytokeratin 7-positive): a distinct entity? *Histopathology* **75**, 174–184 (2019).
19. Kravtsov, O. et al. Low-Grade Oncocytic Tumor of Kidney (CK7-Positive, CD117-Negative): Incidence in a single institutional experience with clinicopathological and molecular characteristics. *Hum. Pathol.* **114**, 9–18 (2021).
20. Guo, Q. et al. Characterization of a distinct low-grade oncocytic renal tumor (CD117-negative and cytokeratin 7-positive) based on a tertiary oncology center experience: the new evidence from China. *Virchows Arch.* **478**, 449–458 (2021).
21. Davis, C. F. et al. The somatic genomic landscape of chromophobe renal cell carcinoma. *Cancer Cell* **26**, 319–330 (2014).
22. Tjota, M. et al. Eosinophilic Renal Cell Tumors With a TSC and MTOR Gene Mutations Are Morphologically and Immunohistochemically Heterogenous: Clinicopathologic and Molecular Study. *Am. J. Surg. Pathol.* https://doi.org/10.1097/PAS.0000000000001457 (2020).
23. Tjota, M. Y., Wanjari, P., Segal, J. & Antic, T. TSC/MTOR-mutated eosinophilic renal tumors are a distinct entity that is CK7+/CK20-/vimentin-: a validation study. *Hum. Pathol.* **115**, 84–95 (2021).
24. Tong, K. & Hu, Z. FOXI1 expression in chromophobe renal cell carcinoma and renal oncocytoma: a study of The Cancer Genome Atlas transcriptome-based outlier mining and immunohistochemistry. *Virchows Arch.* **478**, 647–658 (2021).
25. Skala, S. L. et al. Next-generation RNA Sequencing-based Biomarker Characterization of Chromophobe Renal Cell Carcinoma and Related Oncocytic Neoplasms. *Eur. Urol.* **78**, 63–74 (2020).
26. Saxton, R. A. & Sabatini, D. M. mTOR Signaling in Growth, Metabolism, and Disease. *Cell* **168**, 960–976 (2017).
27. Zoncu, R., Efeyan, A. & Sabatini, D. M. mTOR: from growth signal integration to cancer, diabetes and ageing. *Nat. Rev. Mol. Cell Biol.* **12**, 21–35 (2011).
28. Kim, L. C., Cook, R. S. & Chen, J. mTORC1 and mTORC2 in cancer and the tumor microenvironment. *Oncogene* **36**, 2191–2201 (2017).
29. Huang, J. & Manning, B. D. The TSC1-TSC2 complex: a molecular switchboard controlling cell growth. *Biochem. J.* **412**, 179–190 (2008).
30. Tee, A. R., Manning, B. D., Roux, P. P., Cantley, L. C. & Blenis, J. Tuberous sclerosis complex gene products, Tuberin and Hamartin, control mTOR signaling by acting as a GTPase-activating protein complex toward Rheb. *Curr. Biol.* **13**, 1259–1268 (2003).
31. Dibble, C. C. & Cantley, L. C. Regulation of mTORC1 by PI3K signaling. *Trends Cell Biol.* **25**, 545–555 (2015).
32. Paner, G., Amin, M. B., Moch, H. & Störkel, S. Chromophobe renal cell carcinoma. In *WHO Classification of Tumours of the Urinary System and Male Genital Organs*

Vol. 8 (eds Moch, H., Humphrey, P. A., Ulbright, T. M., & Reuter, V. E.) 27–28 (International Agency for Research on Cancer, Lyon, 2016).
33. Hes, O., Moch, H. & Reuter, V. Oncocytoma. In *WHO Classification of Tumours of the Urinary System and Male Genital Organs* Vol. 8 (eds Moch, H., Humphrey, P. A., Ulbright T. M., & Reuter, V. E) 43–44 (International Agency for Research on Cancer, Lyon, 2016).
34. Petersson, F., Gatalica, Z., Grossmann, P., Perez Montiel, M. D., Alvarado Cabrero, I. & Bulimbasic, S. et al. Sporadic hybrid oncocytic/chromophobe tumor of the kidney: a clinicopathologic, histomorphologic, immunohistochemical, ultrastructural, and molecular cytogenetic study of 14 cases. *Virchows Arch.* **456**, 355–365 (2010).
35. Trpkov, K. et al. Novel, emerging and provisional renal entities: The Genitourinary Pathology Society (GUPS) update on renal neoplasia. *Mod. Pathol.* **34**, 1167–1184 (2021).

AUTHOR CONTRIBUTIONS

Contributions of the authors were as follows: drafting the manuscript: SKMo, SRW. Critical revision and final approval of the manuscript: all authors. Data collection, analysis, and interpretation: all authors. Conception/design: SKMo, SRW.

COMPETING INTERESTS

The authors declare no competing interests.

ETHICS APPROVAL/CONSENT TO PARTICIPATE

The study was approved by the Institutional Review Board of the Advanced Medical Research Institute. Informed consent was waived due to the retrospective nature of the study.

ADDITIONAL INFORMATION

Correspondence and requests for materials should be addressed to Sean R. Williamson.